EFFECT OF POWDER DENSITY VARIATION ON PREMIXED Ti-6Al-4V AND Cu COMPOSITES DURING LASER METAL DEPOSITION

Mutiu F. Erinosho[1], Esther T. Akinlabi[1], Sisa Pityana[2]

[1]Department of Mechanical Engineering Science, University of Johannesburg, Auckland Park Kingsway Campus, Johannesburg, 2006, South Africa.
[2]National Laser Centre, Council for Scientific and Industrial Research (CSIR), Pretoria, 0001, South Africa.

Keywords: Powder density, Laser metal deposition, Microhardness, Microstructure, Ti-6Al-4V/Cu composites

Abstract

This paper reports the effect of powder density variation on the premixed Ti-6Al-4V/Cu and Ti-6Al-4V/2Cu Composites. Two sets of experiment were conducted in this study. Five deposits each were made for the two premixed composites. Laser powers were varied between 600 W and 1700 W while a scanning speed of 0.3 m/min is kept constant throughout the experiment. Investigations were conducted on the microstructures and microhardness of the laser deposited premixed Ti-6Al-4V/Cu and Ti-6Al-4V/2Cu composites. It was found that the evolving microstructures of the composites were characterised with the formation of macroscopic banding and Widmanstatten; and disappears as it grows towards the fusion zone (FZ) and this could be attributed to the changes in the distribution of heat input. Sample A2 of premixed Ti-6Al-4V/Cu composite gives the highest hardness of 393 ± 6.36$VHN_{0.5}$ while sample B4 of premixed Ti-6Al-4V/2Cu composites depicts the highest hardness value of 373 ± 9.18$VHN_{0.5}$.

Introduction

Ti-6Al-4V alloy is a light metal that is mostly applicable in the aerospace and other industries such as chemical, industrial, energy, sport and automotive industrial services since it demonstrates a permutation of physical, mechanical, and corrosion resistance. It also finds application in the bio-medicals due to the possession of excellent biocompatibility among metallic materials [1-2]. The alloys also offer attractive elevated temperature properties for application in hot gas turbine and auto engine components, where more creep-resistant alloys can be selected for temperatures as high as 600 °C and also serves as the keys to improved performance in the aerospace and terrestrial systems [3-5]. Copper (Cu) alternatively, is a beta stabilizer and has a very good control on the microstructures of a composite with the Cu additive. The structure causes a transformation in the graphite phase and boosts the reaction of titanium [6]. The interaction between the process parameters used in laser metal deposition (LMD) is a very intricate task and complicated to apprehend [7, 8]. Disparities in the particle density of a powder cause segregation [9]. The segregation of coarse particle size towards the top of a layer can improve screening efficiency of the powder. Agglomeration processes took advantage of segregation of large agglomerates to enhance the preferential discharge of the powder. The mixing of micro powders by diffusion means in a free-flow requires the movement of individual particles to be random and independent of the type of particle. Thus, the particles should experience the same mobility and if otherwise, segregation prevails within the powder particles [10]. The properties of low-cost powder metallurgy titanium alloys were sintered with 430 stainless steel powder. The density of the mixed powders was increased with the density of stainless steel which was heavier than that of titanium. Thus, the addition of the spherical stainless steel powder to titanium improves the compressibility and prevents the formation of TiFe intermetallic [11]. The surface modification of Ti-6Al-4V substrate was conducted using mixed TiC and Ti powders in the ratio of 1 to 3. The powders were pressed in order to remove the gases between the particles of the powder. It was discovered that the distribution of Ti, V and C are relatively homogeneous. The mass fraction of Al was relatively heterogeneous and was dispensed only between the TiC dendrites [12]. The particle size distribution and shape of powders were put into consideration when TiZrNbMoV alloy was blended and deposited using the Laser Engineered Net Shaping (LENS). It was reported that during the laser deposition process, a homogenous powder flow into the melt pool was difficult to obtain. The report shows that the metal powders to be used in the LENS systems should exhibit a spherical shape with sizes between 40 to 150 microns so as to give a better homogenous powder flow from the powder hopper to the exit nozzles and into the melt pool itself [13].

The motivation for this work is to study the effect of powder density variation on the premixed Ti-6Al-4V and Cu composites during the LMD process. Here, the reasons behind segregation of the two powders after premixing and laser deposition have been investigated. Characterizations were also conducted on the evolving microstructures and microhardness of the premixed Ti-6Al-4V/Cu and Ti-6Al-4V/2Cu composites. The calculations involved in determining the powder flow rate (PFR) used in this experiment were also established.

Experimental methods

The LMD process of the composites was conducted on a fiber laser, Ytterbium Laser System equipment (YLS-2000-TR) powered at 2 kW and uses a Kuka robot for its action and operation. The research work was fascinated at the National Laser Centre of Council of Scientific Industrial Research (NLC-CSIR), Pretoria, South Africa. Figure 1 shows a typical schematic view of a robotic laser with the nozzle attached to the laser head and showing the deposition process with the laser beam. A 99.6 % sandblasted Ti-6Al-4V substrate with dimensions 102 mm X 102 mm X 7.45 mm was prepared for the laser deposition process.

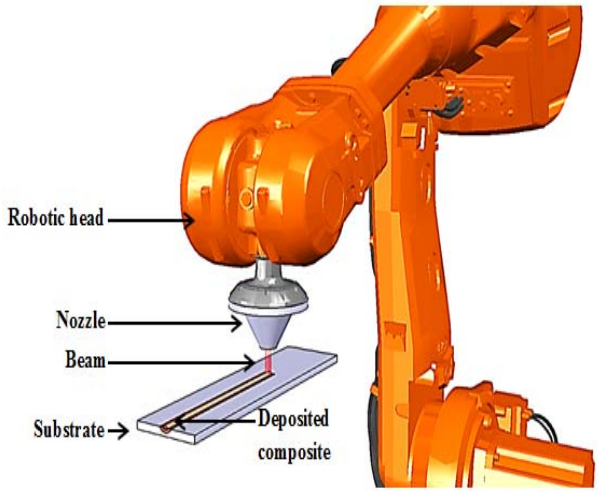

Figure 1. A typical schematic view of a robotic laser

A 12 mm distance is kept between the nozzle and the substrate and the focal length of 210 mm was used throughout the experiment. Trial experimental runs were performed with a mixture of Ti-6Al-4V and Cu powder. One weight percent (1 wt %) of Cu powder was added to 99 wt % of Ti-6Al-4V. Also, another 2 wt % of Cu powder was added to 98 wt % of Ti-6Al-4V powder separately. Figure 2 depicts the Turbula mixer that was used for premixing the powders.

Figure 2. Turbula mixer

The mixtures of different percentage weight of the powders in two different bottles were premixed in the Turbula machine at a speed of 47 rev/min for 5 hours. The required percentage ratios of the powders were measured in a UNIBLOC SHIMADU AUW220D digital reading balance with a maximum capacity of 220 g. The density of Ti-6Al-4V powder is one half (1/2) that of Cu powder. The premixed Ti-6Al-4V/Cu powders were poured into a single hopper prior to laser deposition.

Tables I and II show the process parameters for the premixed Ti-6Al-4V/Cu and Ti-6Al-4V/2Cu composites. The laser powers were varied between 600 W and 1700 W while all other process parameters such as the scanning speed at 0.3 m/min; powder flow rate at 2.1 rpm for Ti-6Al-4V/Cu composites; powder flow rate at 2.0 rpm for Ti-6Al-4V/2Cu composites; and gas flow rate at 1.5 l/min were kept constant.

Table I. Experimental matrix for the premixed Ti-6Al-4V/Cu composites

Sample Designation	Laser Power (W)	Scanning Speed (m/min)	Powder Flow Rate PFR (rpm)	Gas Flow Rate GFR (l/min)
A1	600	0.3	2.1	1.5
A2	900	0.3	2.1	1.5
A3	1200	0.3	2.1	1.5
A4	1500	0.3	2.1	1.5
A5	1700	0.3	2.1	1.5

Table II. Experimental matrix for the premixed Ti-6Al-4V/2Cu composites

Sample Designation	Laser Power (W)	Scanning Speed (m/min)	Powder Flow Rate PFR (rpm)	Gas Flow Rate GFR (l/min)
B1	600	0.3	2.0	1.5
B2	900	0.3	2.0	1.5
B3	1200	0.3	2.0	1.5
B4	1500	0.3	2.0	1.5
B5	1700	0.3	2.0	1.5

Five deposits were made on the sandblasted Ti-6Al-4V substrate using the process parameters and labelled A1 to A5 for Ti-6Al-4V/Cu composites and B1 to B5 for Ti-6Al-4V/2Cu composites. The deposited composites were wire brushed after the deposition process to remove the flux of the laser beam and the unmelted powders. After the deposition, Cu powders were observed to settle down at the bottom of the hopper thereby segregating from Ti-6Al-4V powder. This segregation was detected during the discharging of the last powders from the hopper to the powder container. This occurrence was as a result of the different densities that exist between the two powders. In other word, the particle sizes of Cu powders are greater than that of Ti-6Al-4V powder used. The samples were prepared for grinding, polishing and etching according to E3-11 ASTM standard for metallurgical preparation of samples [14].

Microstructure

The Kroll's reagent was prepared with 100 ml H_2O, 2.5 ml HF and 4.5 ml HNO_3 prior to optical microscopy observation. The reagent was prepared according to Struers application note of metallurgical preparation of titanium (Accessed from the website, 2013) [15]. The samples were etched for 9 - 12 seconds, bathed under clean running water and dried off. The microstructures of the etched samples were observed under the BX51M Olympus optical microscope.

Hardness Tests

The microhardness characterization was conducted on the premixed Ti-6Al-4V/Cu and Ti-6Al-4V/2Cu composites using the Zwick/Roell Vickers hardness machine. Indentations were done on each sample from sample A1 to A5 and B1 to B5 respectively. A load of 500 g and a dwell time of 15 seconds were used throughout the hardness tests according to E384 -11e1 ASTM standard [16].

Determination of powder flow rate used

The calculations required for selecting the PFR are highlighted below. Only 99 wt % Ti-6Al-4V and 1 wt % Cu (Ti-6Al-4V/Cu) is taking into consideration. A similar way can be followed to determine the PFR used for 98 wt % Ti-6Al-4V and 2 wt % Cu (Ti-6Al-4V/2Cu) powders respectively.

From the relationship given in equation 1,

$$\text{Density } \rho = \frac{\text{mass (m)}}{\text{volume(v)}} \tag{1}$$

From the density relationship derived, the volumes of the premixed 99 wt % Ti-6Al-4V and 1 wt % Cu (Ti6Al4V/Cu) powders are presented in equation 2 and 3,

$$V_{T64\rightarrow 99} = \frac{M_{T64\rightarrow 99}}{\rho_{T64}} \tag{2}$$

$$V_{Cu\rightarrow 1} = \frac{M_{Cu\rightarrow 1}}{\rho_{Cu}} \tag{3}$$

Where the $V_{T64\rightarrow 99}$ and $V_{Cu\rightarrow 1}$ are the volumes of 99 wt % Ti6Al4V and 1 wt % Cu powders.

The total volume of mixture $V_{Tm\rightarrow 99+1}$ gives the summation of the two volumes as expressed in equation 4;

Thus,

$$V_{Tm\rightarrow 99+1} = V_{T64\rightarrow 99} + V_{Cu\rightarrow 1} \tag{4}$$

The volume fractions of the two powders are calculated from the relationship in equation 5 and 6.

$$f_{T64\rightarrow 99} = \frac{V_{T64\rightarrow 99}}{V_{Tm\rightarrow 99+1}} \tag{5}$$

$$f_{Cu\rightarrow 1} = \frac{V_{Cu\rightarrow 1}}{V_{Tm\rightarrow 99+1}} \tag{6}$$

Where $f_{T64\rightarrow 99}$ and $f_{Cu\rightarrow 1}$ are the volume fractions of 99 wt % Ti6Al4V and 1 wt % Cu powders respectively. The density of the mixture (Ti6Al4V and Cu) powders gives the expression in equation 7

$$\rho_{Tm\rightarrow 99+1} = \rho_{T64\rightarrow 99} f_{T64\rightarrow 99} + \rho_{Cu\rightarrow 1} f_{Cu\rightarrow 1} \tag{7}$$

Where $\rho_{Tm\rightarrow 99+1}$ is the total density of the premixed powders.

The mass of the total mixture gives the multiplication of the total volume and density of the mixture as presented in equation 8.

$$M_{T64\rightarrow 99+1} = V_{T64\rightarrow 99+1} * \rho_{Tm\rightarrow 99+1} \tag{8}$$

Where $M_{T64\rightarrow 99+1}$ is the mass of the total mixture.
The PFR can be calculated using the expression in equation 9.

$$\text{PFR} = \frac{\text{Mass of deposit}}{\rho_{Tm\rightarrow 99+1} * \text{Time taken}} \tag{9}$$

The time taken can be calculated from the relationship as illustrated in equation 10.

$$\text{Scan speed} = \frac{\text{Deposit track length}}{\text{Time taken}} \tag{10}$$

A constant scan speed of 0.3 m/min and a track length of 50 mm were considered for the deposition processes. The time taken obtained from equation 10 can be substituted in equation 9.

Results and discussion

The results from the trial runs are presented from Ti-6Al-4V/Cu and Ti-6Al-4V/2Cu composites. The microstructural evaluation and the microhardness characterizations are presented and discussed in this section.

Figures 3(a) and (b) show the SEM morphologies of Ti-6Al-4V and Cu powders.

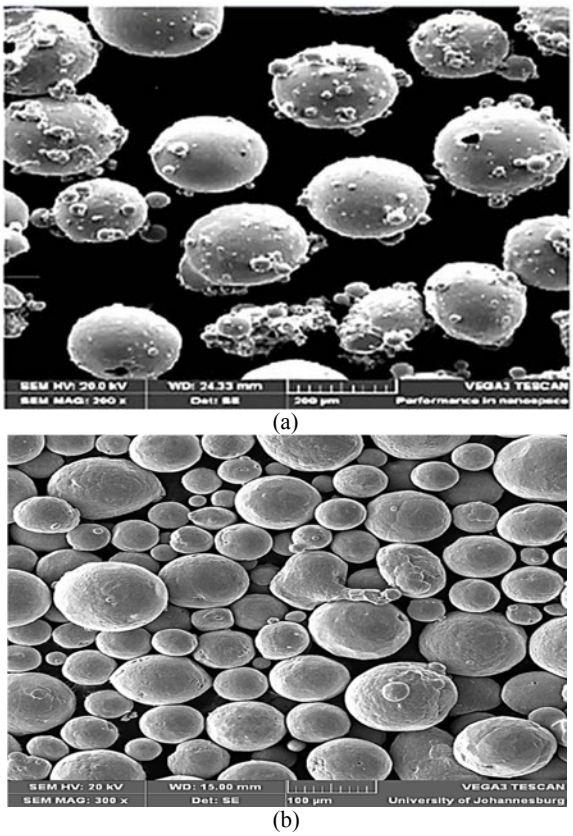

(a)

(b)

Figure 3. The SEM morphology of (a) Ti-6Al-4V powder; (b) Cu powder

Both the Ti-6Al-4V and Cu powders show spherical morphologies. The Ti-6Al-4V powders were detected to have similar shapes and sizes. Smaller particles of 45 µm to 55 µm were found to cling to the bigger particles whilst the Cu powders exhibit similar shapes but different particle sizes. The morphology of Ti-6Al-4V powder shows that the particles are with core and outer wall as shown in Figure 3 (a). This evidence is based on the holes observed on some of the dent particles. The Cu powder shows a rigid morphology and shows a sign of being denser than the titanium powder.

Figures 4 (a) and (b) present the macrographs of the premixed Ti-6Al-4V/Cu and Ti-6Al-4V/2Cu composites deposited at a laser power of 900 W and scanning speed of 0.3 m/min.

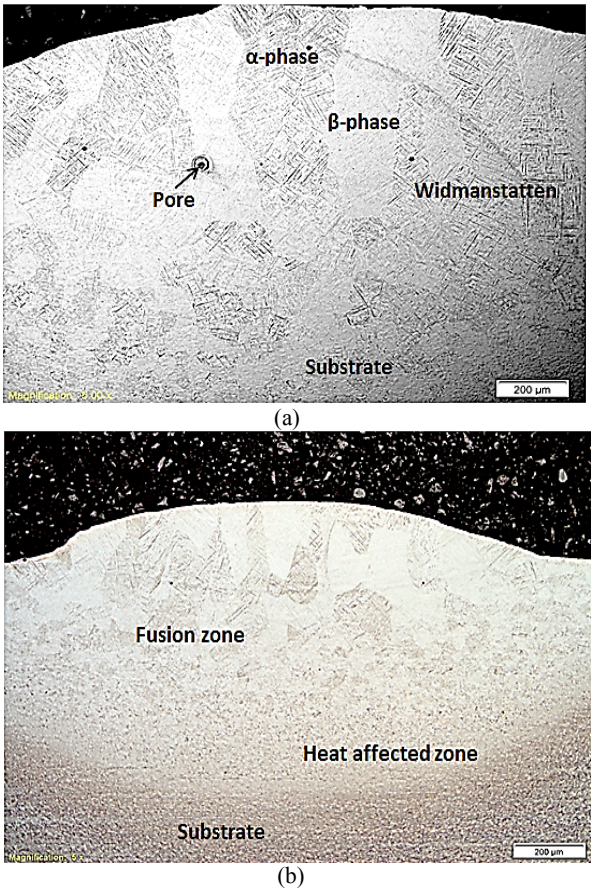

Figure 4. Macrograph of the premixed composites deposited at a laser power of 900 W and a scanning speed of 0.3 m/min (a) sample A2; Ti-6Al-4V/Cu composite (b) sample B2; Ti-6Al-4V/2Cu composite

Investigation of the macrographs of sample A2 of Ti-6Al-4V/Cu composite and sample B2 of Ti-6Al-4V/2Cu composite. In figures 4 (a) and (b) show the formation of macroscopic banding which disappears near the fusion zone (FZ); and the heat affected zone (HAZ). Grains grow epitaxially towards the FZ and HAZ from the freshly nucleated grains into the substrate. There is also the formation of globular structures below the FZ as the laser power increases [17, 18]. The grain boundaries formed at the deposit were wider and laterally terminate as they grow toward the FZ and the HAZ and the occurrence was due to the variation in the distribution of the heat input as the heat travels from the top of the deposit to the FZ and then to the HAZ.

Figures 5 (a) and (b) show the microstructures of premixed Ti-6Al-4V/2Cu composites of sample B3 deposited with a laser power of 1200 W and sample B4 deposited with a laser power of 1500 W respectively.

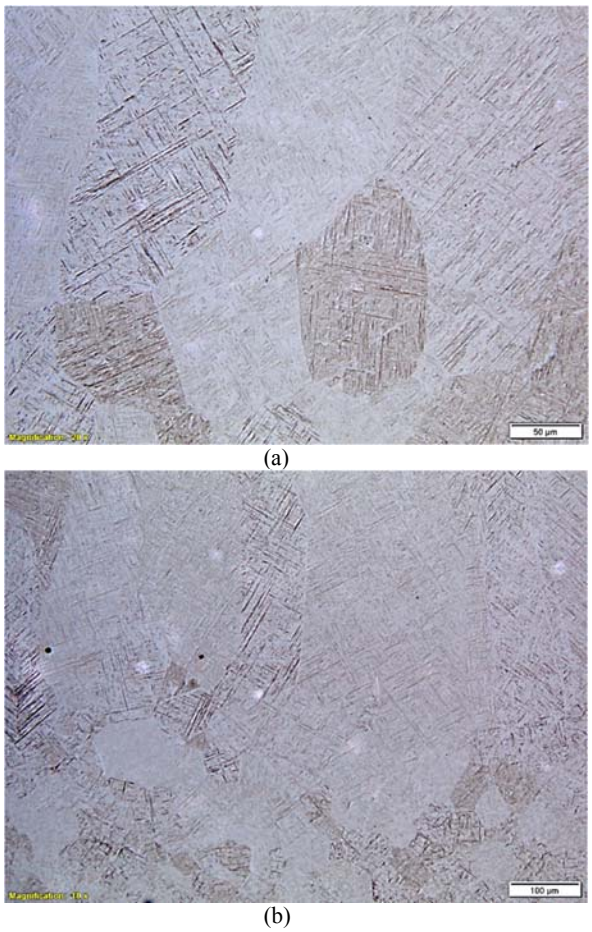

Figure 5. Microstructures of the premixed Ti-6Al-4V/2Cu composites (a) sample B3 at a laser power of 1200 W (b) sample B4 at a laser power of 1500 W

There is formation of Widmanstatten structures in almost all the microstructures due the high cooling rate following solidification [17]. The Widmanstatten structures consist of two phases which are the α-phases and the β-phases. The β-phases were observed to be the white phases and appear finer due to the rate of cooling. The thinness ribs of the β-phase are more due to the alloy composition and thermodynamics. The α-phases were observed to be the dark phases. The rate of the epitaxial growth of the β-phases depends on the rate at which the heat input diffuses within the laser deposited site.

The microhardness evaluations of the premixed Ti-6Al-4V/Cu and Ti-6Al-4V/2Cu composites are presented. The hardness measurements were made on all samples from lots A and B respectively and the results are as shown in Figure 6.

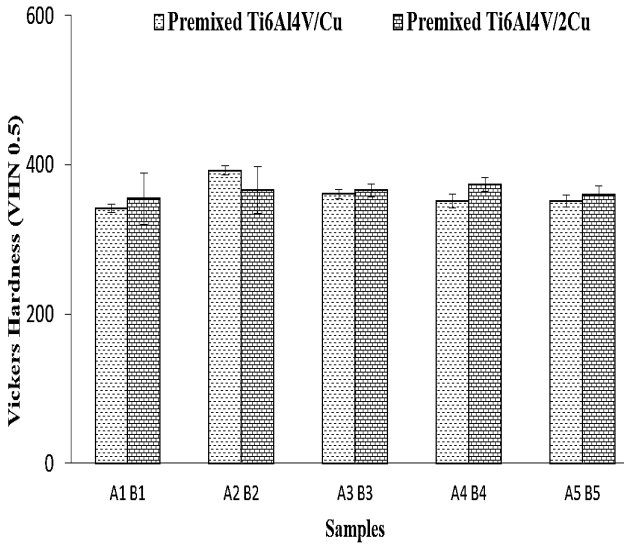

Figure 6. Hardness values of premixed laser deposited composites

Sample A2 of the premixed Ti-6Al-4V/Cu composite gives the highest hardness value with standard deviation of 393 ± 6.36$VHN_{0.5}$ while sample A1 gives the lowest hardness value with standard deviation of 342 ± 5.07$VHN_{0.5}$. From the premixed Ti-6Al-4V/2Cu composites, sample B4 gives the highest hardness value with standard deviation of 373 ± 9.18$VHN_{0.5}$ while sample B1 gives the lowest hardness value with standard deviation of 355 ± 34.51$VHN_{0.5}$. The hardness values increased to a peak point as the laser power increases; and show a decrease in the trend as the laser power continues to decline. This statement was in agreement with [17] when the effect of laser power on the microhardness of Ti-6Al-4V/Cu composites was studied. The hardness values obtained indicate that the process or approach involved in producing a component with similar material is dependent on the alteration of its property. The hardness value of the primary composite was not that improved due to the fact that the Cu powders were noticed to settle down at the bottom of the powder feeder groove and segregate from the otherg powder. Segregation of powders occurs when the motion of the individual particles is predisposed according to the size, shape, composition of the powders [10]. Ideally, the density of Cu is twice the density of Ti-6Al-4V alloy and by considering the particle sizes of the two powders used, Cu powder exhibit larger particle size as compared to Ti6Al4V alloy. The hardness results obtained justify the advantage of using two separate hoppers when compared to the work conducted by [17] on Ti-6Al-4V/Cu composites. However two hoppers would be more appropriate in order to reduce or eliminate the problem of segregation. Equation 10 can be used to determine the mass of each of the deposited composites at varying PFR while keeping all other parameters constant. Once the scanning speed and the length of deposited tracks are known, the time of deposit can be calculated.

Conclusion

The deposition of Ti-6Al-4V/Cu composites from the premixed powders was conducted and investigated. Although, segregation of the powders was observed due to the differences in the powder densities and the particle sizes of both the Ti-6Al-4V and Cu powders. Characterizations were carried out on the microstructures and microhardness of the deposited composites. The macroscopic banding was formed in the fusion zone and became less pronounced; and eventually disappeared in the heat affected zone. The rate of the epitaxial growth of the both the α-phases and β-phases depends on the rate at which the heat input diffused into the composites. The formulas obtained can be used in determining the mass of each deposited composites at varying powder flow rate while keeping all other parameters constant.

Acknowledgement

This work is assisted and supported by the Rental Pool Programme of National Laser Centre, Council of Scientific and Industrial Research (CSIR), Pretoria, South Africa. Acknowledgement also goes to the African Laser Centre for the bursary award to Mr Erinosho M F.

Reference

[1] Moiseyev V. N, *Titanium alloys: Russian aircraft and aerospace applications* (CRC Press Taylor & Francis Group, 2006), 169-180.

[2] Lutjering G, Williams J.C, *Titanium, Springer*, (2nd edition, printed book, 2007).

[3] Congress of the U.S. office of Technology Assessment, *"Advanced Materials by Design-Polymer Matrix Composite"*, (OTA-E-351, Washington, June 1988), 83-85.

[4] Francis H. Froes, Te-Lin Yau and Hans G. Weidenger, "Titanium, Zirconium and Hafnium" Chapter 8, Materials Science and Technology – (MKJ Structure and Properties of Nonferrous Alloys, vol. ed. K.H. Matucha, VCH Weinheim, FRG, 1996), 401.

[5] Boyer R. R, Welsch, G and Collings E. W, Eds. "*Materials Properties Handbook: Titanium Alloys*", (ASM Int., Materials Park, OH.r–2Nbbypressureless sintering, 1994).

[6] X. H. Zhang, M. H. Yu, H. Q. Tang and G. C. Su, "Effect of copper addition on microstructures and mechanical properties of in situ TiCp/Fe composites," *Materials and Design*, 32 (6) (2011), 3560-3565.

[7] S. Bontha, "The Effect of Process Variables on Microstructure in Laser-Deposited Materials," (PhD thesis, Wright State University, Engineering, 2006).

[8] E. Brandl, A. Schoberth and C. Leyens, "Morphology, microstructure, and hardness of titanium (Ti-6Al-4V) blocks deposited by wire-feed additive layer manufacturing (ALM)," *Materials Science and Engineering*, 532 (2012), 295-307.

[9] Vallance, J.W. and Savage, S.B. *Particle Segregation in Granular Flows down Chutes,* (IUTAM Symposium on Segregation in Granular Flows, A.D. Rosato and D.L. Blackmore, eds., Kluwer Academic Publishers, Boston, 2000), 31-51.

[10] R. Hogg, "Mixing and Segregation in Powders: Evaluation, Mechanisms and Processes," *KONA Powder and Particle Journal*, 4 (27) (2009), 3-17.

[11] L. Bolzoni, E. Herraiz, E. M. Ruiz-Navas and E. Gordo, "Study of the properties of low-cost powder metallurgy titanium alloys by 430 stainless steel addition," *Materials & Design*, 60 (2014), 628-636.

[12] K. Zhang, J. Zou, J. Li, Z. Yu and H. Wang, "Surface modification of TC4 Ti alloy by laser cladding with TiC+Ti powders," *Transactions of Nonferrous Metals Society of China*, 20, (11) (2010), 2192-2197.

[13] I. Kunce, M. Polanski, J and Bystrzycki, "Microstructure and hydrogen storage properties of a TiZrNbMoV high entropy alloy synthesized using Laser Engineered Net Shaping (LENS)," *International Journal of Hydrogen Energy*, 39, (18) (2014), 9904-9910.

[14] E3-11 Standard Guide for Preparation of Metallographic Specimens, (ASTM International, 2011).

[15] Struers Application Note on Titanium. http://www.struers.com/resources/elements/12/104827/ Application_Note_Titanium _English.pdf. Accessed 2013.

[16] ASTM E384 - 11e1, *Standard Test Method for Knoop and Vickers Hardness of Materials*, (ASTM International Book of Standards, 03, (01) (2011).

[17] M. F Erinosho, E. T Akinlabi and S. Pityana, "Laser Metal Deposition of Ti6Al4V/Cu Composite: A Study of the Effect of Laser Power on the Evolving Properties," *Proceedings of the World Congress on Engineering*, II, (2014), 1203-1208.

[18] M. Shukla, R. M. Mahamood, E. T. Akinlabi and S. Pityana, "Effect of Laser Power and Powder Flow Rate on Properties of Laser Metal Deposited Ti6Al4V". *World Academy of Science, Engineering and Technology, International Journal of Mechanical, Industrial Science and Engineering,* 6, (11) (2012), 38.